AIP | Journal of Applied Physics

Phase diagram and spin-glass phenomena in electron-doped La1xHfxMnO3 (0.05x0.3) manganite oxides

E. J. Guo, L. Wang, Z. P. Wu, L. Wang, H. B. Lu et al.

Citation: J. Appl. Phys. **110**, 113914 (2011); doi: 10.1063/1.3666056
View online: http://dx.doi.org/10.1063/1.3666056
View Table of Contents: http://jap.aip.org/resource/1/JAPIAU/v110/i11
Published by the American Institute of Physics.

Phase diagram and spin-glass phenomena in electron-doped $La_{1-x}Hf_xMnO_3$ ($0.05 \le x \le 0.3$) manganite oxides

E. J. Guo,[1,2] L. Wang,[1] Z. P. Wu,[1] L. Wang,[2] H. B. Lu,[2] K. J. Jin,[2] and J. Gao[1,a)]
[1]*Department of Physics, The University of Hong Kong, Pokfulam Road, Hong Kong*
[2]*Beijing National Laboratory for Condensed Matter Physics, Institute of Physics, Chinese Academy of Sciences, Beijing 100190, People's Republic of China*

(Received 24 August 2011; accepted 9 November 2011; published online 9 December 2011)

The effects of tetravalent hafnium doping on the structural, transport, and magnetic properties of polycrystalline $La_{1-x}Hf_xMnO_3$ (LHMO) ($0.05 \le x \le 0.3$) were investigated systematically. LHMO exhibited a typical colossal magnetoresistance effect via the double-exchange between Mn^{2+} and Mn^{3+} ions, instead of that between Mn^{3+} and Mn^{4+} ions in hole-doped manganites. A phase diagram was obtained for the first time through magnetization and resistance measurements in a broad temperature range. As the Hf concentration varied from $x = 0.05$ to 0.3, the Curie point and metal-to-insulator transition temperature increased significantly, whereas the magnetization and resistivity decreased remarkably. An abnormal enhancement of the magnetization was observed at about 42 K. It was further confirmed that a second magnetic phase MnO_2 in LHMO gives rise to such a phenomenon. The possible causes are discussed in detail. The dynamic magnetic properties of LHMO, including relaxation and aging processes, were studied, demonstrating a spin-glass state at low temperature accompanied by a ferromagnetic phase. © *2011 American Institute of Physics*. [doi:10.1063/1.3666056]

I. INTRODUCTION

One of the current interests in condensed matter physics is the investigation of strong electronic correlation in transition metal oxides. In doped manganites, the interactions among charge, orbital, spin, and lattice result in a variety of intriguing phenomena, such as colossal magnetoresistance (CMR),[1,2] charge-orbit-ordering,[3,4] and high-temperature superconductivity.[5,6] The parent compound $LaMnO_3$ is a charge-transfer insulator with trivalent manganese in different layers that couple themselves anti-ferromagnetically through a superexchange (SE) mechanism. But within a layer, these Mn^{3+} ions are coupled ferromagnetically. Usually, doping divalent elements in manganites, such as Sr,[3,7–10] Ca,[11,12] and Ba,[13] can introduce holes in the e_g band via the partial substitution of a proportionate amount of Mn^{3+} ions (with the electronic configuration $t_{2g}^3 e_g^1$ and total spin $S = 2$) with Mn^{4+} ions (t_{2g}^3, single localized spin $S = 3/2$). The holes can be permitted charge transfer in the e_g orbital, which has a strong hybridization with the $2p$ state of a neighboring oxygen ion. As a result, due to the intra-atomic Hund's rule, hopping of the e_g electrons can induce ferromagnetic coupling between Mn^{3+} and Mn^{4+} ions. It is responsible for the ferromagnetism and the associated metallic conductivity in the doped manganite oxides. Meanwhile, the reduction in the disorder of the manganese spins will cause a decrease in resistivity and lead to a metal-to-insulator transition (MIT) around the Curie temperature (T_C). The double-exchange (DE) mechanism and strong electron-phonon interaction arising from Jahn-Teller distortion were introduced in order to fully clarify the origin of the CMR effect.[7–11]

Following the study of Das *et al.*,[14] many researchers attempted to substitute tetravalent Ce^{4+}, Te^{4+}, Sn^{4+}, and Sb^{4+} ions at the La site in order to gain electron doped manganite oxides.[14–24] Their results revealed that the physical and chemical properties are strongly dependent on the doped elements and doping level. It is generally believed that these so-called electron-doped manganites exhibit the CMR effect via the DE between Mn^{3+} and Mn^{2+} ions, instead of DE between Mn^{3+} and Mn^{4+} ions as in hole-doped compounds.[14,23] This creates the possibility of fabricating all manganite *p-n* junctions and spintronic devices in the near future. However, as many tetravalent elements can show multivalent states, arguments can be raised as to whether it is intrinsically electron-type or hole-type for the conductive mechanism in a tetravalent ion doped $LaMnO_3$ system. Unlike other tetravalent elements, Hf typically shows a single tetravalent state or zero. This makes studies of the electronic structure of the $La_{1-x}Hf_xMnO_3$ system relatively simple and more reliable. On the other hand, the radius of the Hf^{4+} ion lies intermediately among commonly used dopants [Sn^{4+}(0.081 nm) < Hf^{4+}(0.083 nm) < Ce^{4+}(0.097 nm) < La^{3+}(0.106 nm)]. It is expected that the substitution of La^{3+} by Hf^{4+} might form a similar electron-doped manganite oxide like the others. Recently, Hf doped manganite [$La_{1-x}Hf_xMnO_3$ (LHMO)] was reported by our group.[25–28] Our previous results from x-ray photoemission spectroscopy (XPS) reveal that the LHMO compound is in a mixed valence state of Mn^{2+} and Mn^{3+}, and the magnetic-field dependence of Hall resistivity further confirmed that the carriers in LHMO are electrons. All the results imply the electron conduction mechanism in LHMO.[27] Although the properties of epitaxially grown

a)Author to whom correspondence should be addressed. Electronic mail: jugao@hku.hk.

LHMO thin films have been studied,[25,26,28] there has been no systematic investigation of the physical properties of LHMO bulk materials with different doping levels. In this paper, we investigate the effects of tetravalent Hf doping on the structural, transport, and magnetic properties of polycrystalline LHMO samples. The phase diagram was obtained for the first time through magnetization and resistance measurements. An abnormal enhancement of the magnetization induced by the impurity phase is discussed in detail.

II. SAMPLE PREPARATION AND EXPERIMENTAL DETAILS

Bulk polycrystalline samples of $La_{1-x}Hf_xMnO_3$ ($0.05 \leq x \leq 0.3$) were prepared via the standard solid state reaction method. Stoichiometric amounts of La_2O_3, HfO_2, and MnO_2 high-purity powders were mixed together sufficiently and preheated to 900 °C for 12 h. Then, it was pressed into pellets and sintered in air at 1200 °C for 96 h with intermediate grindings and cooled down to room temperature slowly. A second sintering by repeating the second step was carried out in order to improve the purity of samples. The structure of the LHMO samples was examined via powder x-ray diffraction (XRD) measurements using Cu Kα radiation. The dc magnetization measurements, as a function of temperature (10–300 K) and applied magnetic field (from −5 to +5 T), were carried out. The electrical transport properties were measured via the standard four-probe method. Electric contacts were made using silver paste with a contacting resistance below 0.05 Ω at room temperature. The dc magnetization and resistance of the LHMO samples were measured using a Physical Property Measurement System (PPMS-9 T, Quantum Design). The data acquisition was done in dc mode, which measures the voltage under an alternative dc current, and the sample resistivity is obtained by averaging these signals at each temperature. In this way, the contacting thermal power is naturally removed. The temperature stabilization was better than 0.1%, and the resolution of the voltmeter was better than 10 nV.

III. RESULTS AND DISCUSSIONS

A. Structural analysis

Figure 1(a) shows the XRD $\theta - 2\theta$ scanning curves of LHMO with different Hf doping levels. Almost all main peaks from the samples can be indexed by a rhombohedral structure. As we can find in Fig. 1(a), the peaks from the secondary phase can always be observed when the doping level increases from 0.05 to 0.3. It was further confirmed as the unreacted MnO_2 phase, which is probably due to the difference in ionic radius between La^{3+} (0.106 nm) and Hf^{4+} (0.083 nm). We fitted the XRD data using the software POWDER-X and obtained the lattice parameters of all the LHMO samples. As shown in Fig. 1(b), the doping levels dependent on the *c*-axis and *a*-axis lattice constant of LHMO were presented. It is obvious that the *a*-axis lattice constant shrinks, whereas the *c*-axis expands monotonically with the Hf concentration, which clearly indicates that Hf ions have been successfully substituted into the La sites. A smaller

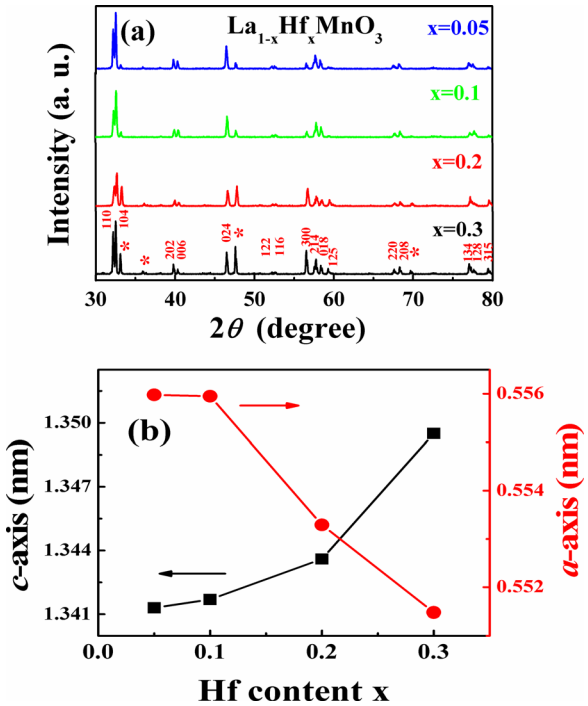

FIG. 1. (Color online) (a) X-ray diffraction $\theta \sim 2\theta$ scanning curves of $La_{1-x}Hf_xMnO_3$ ($0.05 \leq x \leq 0.3$). Almost all main peaks can be indexed by a rhombohedral structure. When $x \geq 0.2$, the second phase MnO_2 can be observed; this is identified in the figures. (b) Doping dependence of the *c*-axis lattice constant and *a*-axis lattice constant showing a common feature: the *a*-axis lattice constant shrinks, whereas the *c*-axis expands monotonically with Hf substitution. This systematic evolution clearly indicates that Hf ions have been successfully substituted into the La sites.

a-axis and larger *c*-axis constant will lead to a decrease in the Mn-O bond length and an increase of the Mn-O-Mn bond angle.[19] Therefore, the MnO_6 octahedral will be distorted. Consequently, both DE and SE interactions will compete more strongly, with dependence on the structural distortion, giving rise to a magnetically disordered state. It can affect the magnetic and electrical transport properties of LHMO dramatically.

B. Resistivity, magnetization, and phase diagram of LHMO ($0.05 \leq x \leq 0.3$)

The magnetic and electrical transport properties of LHMO with different doping levels were investigated. Figure 2(a) shows the temperature dependence of the dc magnetization of LHMO ($x = 0.05$, 0.1, 0.2, and 0.3) under a magnetic field of 200 Oe measured in both zero-field-cooling (ZFC) and field-cooling (FC) modes. All the samples exhibit a paramagnetic (PM) to ferromagnetic (FM) transition behavior. Several explicit effects on the magnetization of LHMO induced by doping with Hf were observed. Firstly, the slope of the magnetization around T_C becomes more pronounced with higher Hf concentrations. Secondly, as the Hf content increases, there is a significant drop in the total magnetization at low temperature and an increase of T_C. The T_C, defined as the peak temperatures in the curves of dM/dT versus temperature, are 170, 180, 230, and 225 K for $x = 0.05$, 0.1, 0.2, and 0.3, respectively. The results might be caused by the competition between the DE and the core spin interaction, which leads

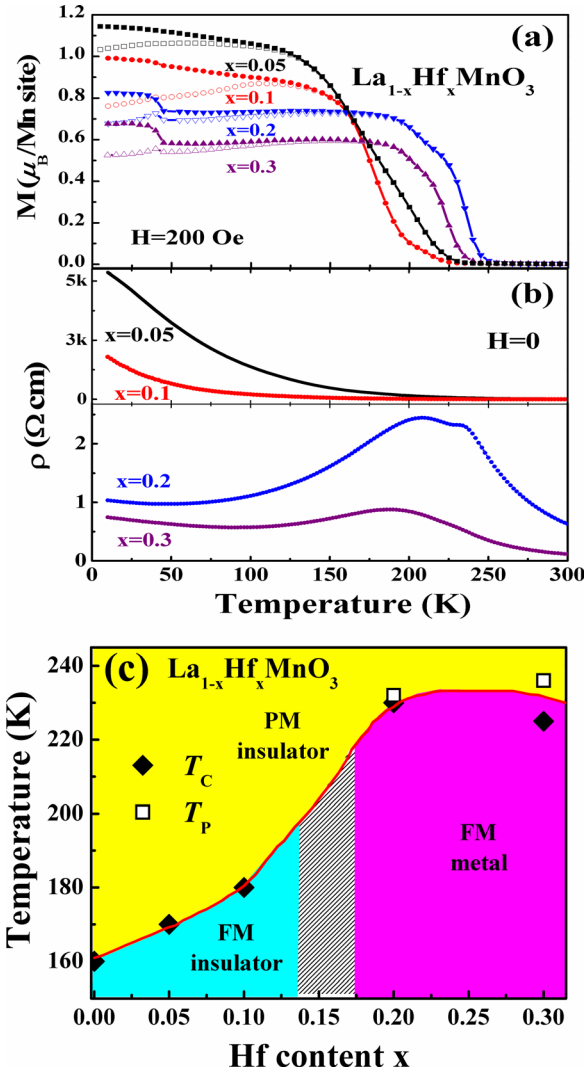

FIG. 2. (Color online) (a) The temperature dependence of magnetization in an applied field of 200 Oe and (b) the temperature dependence of the resistivity (ρ) in zero field. The arrows point out the positions of MIT temperatures. All the measurements were carried out on $La_{1-x}Hf_xMnO_3$ ($0.05 \leq x \leq 0.3$). The magnetization was measured in ZFC (open symbols) and FC (solid symbols) modes. (c) The phase diagram of $La_{1-x}Hf_xMnO_3$, based on the present work. T_P and T_C are taken from (a) *M-T* and (b) ρ-T curves.

to the canting of the core spins as the doping level increases. Thirdly, a bifurcation occurs between the ZFC and FC curves at low temperatures when LHMO is measured in a 200 Oe field. This is a typical spin-glass behavior and can be observed in either hole-doped manganites like $La_{1-x}Sr_xMnO_3$ and $La_{1-x}Ca_xMnO_3$ (Refs. 7–11) or other electron-doped manganites like $La_{1-x}Ce_xMnO_3$ and $La_{1-x}Te_xMnO_3$.[15–21] Moreover, an abnormal enhancement of the magnetization was found at about 40 K when $x \geq 0.1$. It is suggested that an impurity phase mixed in LHMO compounds might give rise to such a phenomenon (a detailed discussion can be found in Sec. III C).

Figure 2(b) displays the temperature dependence of the resistivity (ρ) for the LHMO ($0.05 \leq x \leq 0.3$) without magnetic fields. For $x = 0.05$ and 0.1, the LHMO shows an insulator behavior ($d\rho/dT < 0$) at all temperatures. LHMO with $x = 0.2$ and 0.3 presents a MIT behavior with decreasing temperature. The resistivity of LHMO decreases with increasing doping level x as the result of increasing carriers. We measured the temperature dependence of the resistivity for LHMO (0.2) under various fields of 0, 0.02, 0.1, 0.25, 1, 2, 3, and 5 T, as shown in Fig. 3. At zero magnetic field, the ρ-T curve shows two independent peaks: a sharp peak at higher temperature ($T_{R1} \sim 232$ K) and a broad, larger peak at lower temperature ($T_{R2} \sim 210$ K). Such a shoulderlike feature had also been observed for oxygenated $La_{2/3}Ba_{1/3}MnO_3$ samples[13] and $La_{0.7}Ce_{0.3}MnO_3$ samples.[14] Both of them indicated that the first-order nature of this transition in the vicinity of the double peaks is caused by oxygen overdoping. With increasing magnetic field H, ρ drops dramatically in all temperature ranges. The sharp peak at T_{R1} is gradually suppressed and shifts to higher temperatures with increasing magnetic fields, whereas the position of the peak at T_{R2} has never moved. The inset of Fig. 3 shows the field dependence of T_{R1}. T_{R1} increases from 232 to 280 K when H increases from 0 to 5 T, demonstrating a typical characteristic of CMR materials. It is evident that T_{R1} is the real MIT temperature. The temperature dependence of MR (defined as $MR = [R(0) - R(H)]/R(0) \times 100\%$) for different magnetic fields is also shown in Fig. 3. The MR versus T curves shows a gradual growth peak at T_{R1} with increasing H. The MR values of LHMO(0.2) are 0.59%, 1.92%, 5.79%, 17.96%, 29.66%, 38.91%, and 50.9% under $H = 0.02$, 0.1, 0.25, 1, 2, 3, and 5 T measured at T_{R1}, respectively. The same measurements were carried out in LHMO (0.3) samples, and the MIT temperature of LHMO (0.3) was about 236 K. The Curie temperature T_C from *M-T* curves corresponds with the

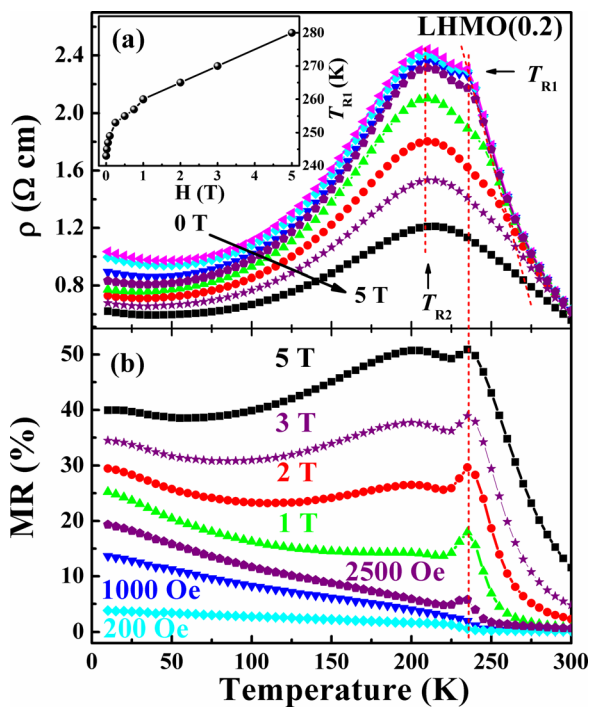

FIG. 3. (Color online) The temperature dependence of the resistivity (ρ) and the magnetoresistance (MR) for LHMO(0.2) under fields of 0, 0.02, 0.1, 0.25, 1, 2, 3, and 5 T. Two vertical red dashed lines are plotted in order to point out two independent temperatures T_{R1} and T_{R2}. The inset shows the field dependence of T_{R1}, demonstrating a typical characteristic of CMR materials.

transition temperatures T_P from ρ-T curves for LHMO with high doping levels. Based on these data, a phase diagram of LHMO as a function of T and Hf content within x = 0.05–0.3 could be obtained, as shown in Fig. 2(c). The T_C of the undoped $LaMnO_3$ compound is about 160 K, as obtained from Schiffer *et al.*[11] The solid line in the figure is a guide for the eye in order to point out the approximate boundary between the spin-disordered PM state and the spin-ordered FM state. As one can see, the hatched area indicates the approximate boundary of the ground states of insulating and metallic conduction modes.

However, one might argue whether LHMO is intrinsically electron-type or hole-type for the conductive mechanism. In our previous works,[26–28] the XPS measurements revealed that the binding energies of the Hf 4f-spectrum in LHMO were found to be about 2 eV greater than that of Hf-metal and almost identical to the 4f binding energies of HfO_2, which suggests that the Hf^{4+} ion is indeed in the tetravalent state in LHMO. At the same time, the shape of the Mn 2p doublet and the value of the Mn 3s exchange splitting provide clear evidence of the presence of Mn^{2+} ions. Thus we conclude that our LHMO film is in a mixed valence state of Mn^{2+} and Mn^{3+}, implying an electron-doped conduction mechanism. Hall effect measurements were also carried out in LHMO. In the strongly correlated systems, although the Hall effect is complex because of the anomalous Hall effect, it is possible to identify the carrier type in terms of the ordinary Hall effect. In ferromagnets, the Hall resistivity contains an additional term that depends on the magnetization,[23]

$$\rho_H = R_0 B + \mu_0 R_S M, \quad (1)$$

$$B = \mu_0 [H + (1 - N)M], \quad (2)$$

where R_0 is the ordinary Hall coefficient, R_S is the anomalous Hall coefficient, M is the magnetization, N is the demagnetization factor, and μ_0 is the vacuum permeability. To separate the two terms, we measured M(H) on the same sample, and M is saturated when $H > 2$ T at 170 K. The second term will not change the slope of ρ_H(H) at high fields. The Hall resistance fit linearly at H > 2 T. The curves for ρ_H(H) at both temperatures exhibit a negative high-field slope, similar to what was reported by Yang *et al.*,[29] implying that the charge carriers in LHMO are electrons.

In addition, one might also doubt that the CMR behaviors observed in our experiments are the result of the creation of oxygen interstitial sites or vacancies at the La sites in our samples. The T_P of LHMO (~230 K) is much higher and the resistivity of LHMO (~10^{-3} to 10^{-4} Ω cm) is several orders of magnitude lower than those of $LaMnO_{3+\delta}$ ($T_p \sim 110$ K and $\rho \sim 10^3$ Ω cm).[30,31] Therefore, we can exclude the effects of $LaMnO_{3+\delta}$ with oxygen deficiency or La-site deficiency on the CMR behaviors. In the generic hole-doped manganite, the CMR effect can be well understood by the DE effects between the Mn^{3+} and Mn^{4+} ions. In the Hf doped manganites, the rare-earth ion is partially replaced by tetravalent Hf^{4+} ions, and the corresponding amount of manganese will be converted into a divalent state. The mixed-valence state of manganese ions in LHMO is Mn^{2+}-Mn^{3+} instead of Mn^{3+}-Mn^{4+}. There are some differences between the hole-doped and electron-doped manganites, such as the electronic configuration being $(t_{2g}^3 e_g^2)$, $(t_{2g}^3 e_g^1)$, and (t_{2g}^3), and the sums of the spin are $S = 5/2$, 2, and 3/2 for Mn^{2+}, Mn^{3+}, and Mn^{4+}, respectively. The 3d state densities of Mn^{4+} and Mn^{2+} are greatly different from each other. All of these lead to the differences between the wavefunction Ψ and the Hamiltonian H when calculating the function of the DE model. Thus, it might be necessary to make some modifications to the DE mechanism, which is well suited for the hole-doped manganites, when it is applied to the electron-doped manganites.

C. Observation of secondary phase in LHMO compounds

In Fig. 2(a), an abnormal enhancement of the magnetization was observed at about 40 K on the LHMO samples when x ≥ 0.1. Similar results were also reported on other electron-doped manganites, such as $La_{1-x}Te_xMnO_3$ and $La_{1-x}Ce_xMnO_3$.[15,19] However, the origin of the enhanced magnetization at low temperatures has not been well understood or discussed. The enhanced magnetization at low temperature is usually attributed to the following things: (i) temperature-induced structure transformation, (ii) spin reorientation in magnetization, and/or (iii) a magnetic impurity phase mixed in manganites. We measured the magnetization of LHMO with x = 0.2 (LHMO(0.2)) under fields of 200 and 1000 Oe in the range of 10–60 K with a step of 1 K, as shown in Figs. 4(a) and 4(b). The measurements were carried

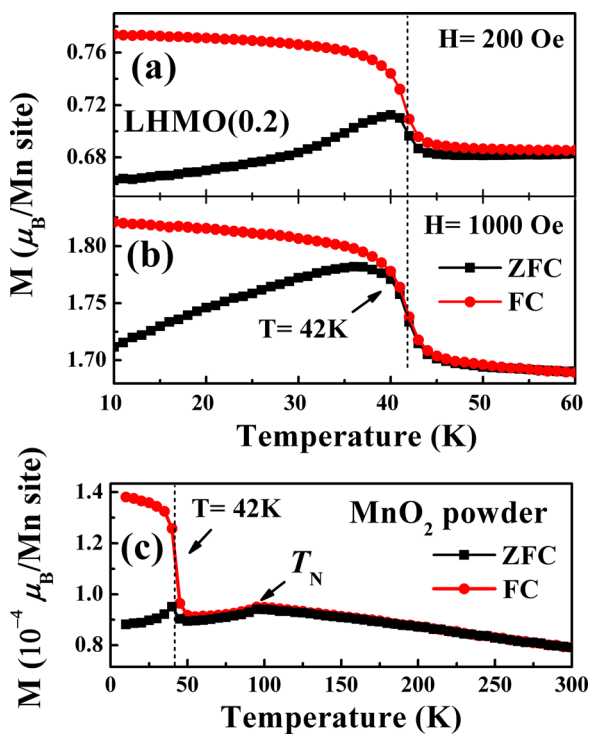

FIG. 4. (Color online) The temperature dependence of the magnetization for LHMO(0.2) in the range of 10–60 K. The measurements were carried out under fields of (a) 200 Oe and (b) 1000 Oe in the ZFC and FC modes. An obvious bifurcation occurs between two measured modes. (c) The temperature dependence of the magnetization for MnO_2 powder in an applied field of 200 Oe. Note that an anomalous enhancement of the magnetization occurs at 42 K in both LHMO and impurity phase MnO_2.

out in ZFC and FC modes. The second transition happened exactly at 42 K, as determined by the peak of dM/dT versus temperature curves. Despite the fact that LHMO(0.2) samples entered the spin-glass state at about 150 K (as shown in Fig. 2(a)), the result shows a larger and significant bifurcation between ZFC and FC curves when the temperature is below 42 K. In Figs. 4(a) and 4(b), it can be found that with increasing temperature, the deviation between ZFC and FC magnetization (ΔM) gradually decreases. With an increase in the external field from 200 to 1000 Oe, ΔM also decreases at the same measuring temperature. This is because the spin-glass state is not at equilibrium with an energy higher than that of the long-range FM equilibrium state. The transition from spin-glass state to FM state should overcome the energy barrier, which will decline gradually with an increase of temperature and magnetic field.

The impurity phases were found in the electron-doped manganites commonly. By intensively analyzing the XRD data of $La_{0.7}Ce_{0.3}MnO_3$, Mitra *et al.*[16] identified the impurity phase in the $La_{0.7}Ce_{0.3}MnO_3$ bulk samples as unreacted CeO_2. Recently, Chou *et al.*[17] further examined the microscopic morphology and composition distribution of $La_{0.7}Ce_{0.3}MnO_3$ and $La_{0.8}Te_{0.2}MnO_3$ bulks. Besides their own phases, the former contains a multiphase of $La_{0.85}Ce_{0.017}MnO_{3+\delta}$, CeO_2, and Mn-O, and the latter contains a lanthanum deficient $La_{0.9}MnO_{3+\delta}$ phase. However, it is hard to understand the abnormal enhancement of the magnetization at low temperature when mixed with nonmagnetic impurity phases of CeO_2 or other perovskite structures. Gebhardt *et al.*[15] have observed a second transition of the magnetization in $La_{1-x}Ce_xMnO_3$ compounds around 40 K, which was attributed to the antiferromagnetic transition arising from unreacted MnO_2. Figure 4(c) presents the magnetization versus temperature scan of MnO_2 powder under 200 Oe field in both ZFC and FC modes. The Néel temperature T_N (~95 K) of MnO_2 powder is indicated in Fig. 4(c). An enhanced magnetization occurs in MnO_2 at the same temperature of 42 K as in the LHMO(0.2) samples. The magnetization of MnO_2 increases suddenly by 40% when the temperature decreases from 45 to 35 K. The bifurcation between ZFC and FC becomes very distinct below 42 K, which coincides with the results found for LHMO(0.2). Therefore, the impurity phase of MnO_2 could provide a big contribution to the total magnetization of LHMO bulks at low temperature.

Figure 5(a) shows the temperature dependence of the magnetization for LHMO(0.2) at magnetic fields of 0.02, 0.1, 1, 2, and 5 T, respectively. Because the ZFC and FC curves match at higher magnetic fields, we present only the results measured in FC modes. The *M-T* curves measured under different fields show a similar trend of FM-PM transition and a slight increase in T_C with increasing fields. It is noteworthy that the enhancement of magnetization at 42 K becomes gradually less obvious with further increasing in field. The reason for this might be that two different magnetic phases are saturated at high magnetic fields. Figure 5(b) presents the field dependence of the magnetization for LHMO(0.2) measured at 10, 45, 150, and 300 K. When the temperature is below $T_C \sim 230$ K, LHMO(0.2) is in a FM state and saturation occurs at relatively low fields. Above T_C,

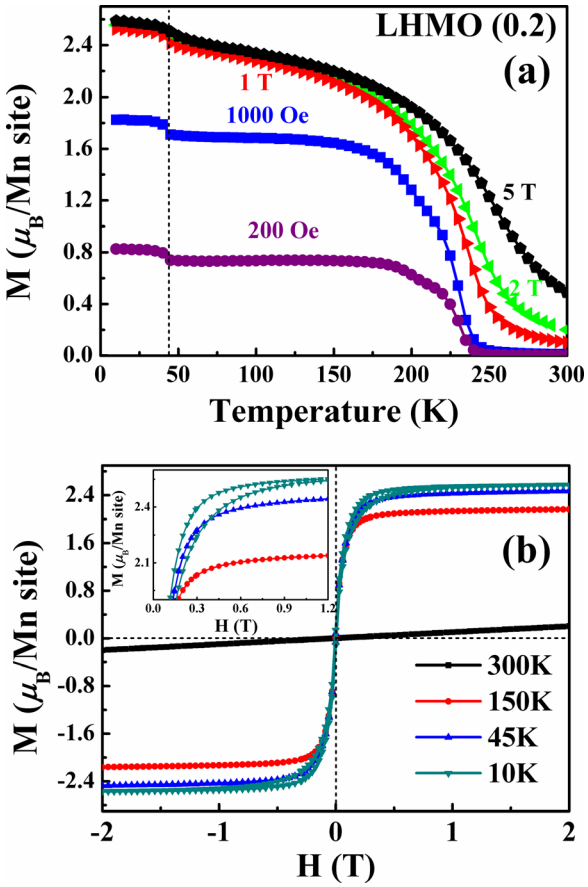

FIG. 5. (Color online) (a) The temperature dependence of the magnetization for LHMO(0.2) at magnetic fields of 0.02, 0.1, 1, 2, and 5 T. The magnetization was measured in FC mode. (b) The field dependence of the magnetization for LHMO(0.2) at constant temperatures of 10, 45, 150, and 300 K. The inset of (b) shows the expanded view of the LHMO(0.2) magnetization curves around the saturation magnetization.

LHMO(0.2) becomes paramagnetic, as demonstrated by the linear relationship of the *M-H* curves measured at 300 K. The inset of Fig. 5(b) shows the expanded view of the LHMO(0.2) *M-H* curves around the saturation magnetization. The *M-H* loop at 10 K shows a different shape than that at 45 K, which demonstrates that the impurity phase MnO_2 plays an important role in the contribution of magnetization due to the different saturated magnetization. We also measured the detailed magnetization of LHMO with $x = 0.05$, 0.1, and 0.3 with the same measurements. In LHMO with $x = 0.05$, no obviously enhanced magnetization can be found. With increasing doping level x, the deviation ΔM between FC and ZFC becomes larger, and the disparity in the *M-H* loops measured at 10 and 45 K becomes bigger. Such phenomena can be attributed to the increasing amount of impurity. The XRD data also confirm our explanation. When the doping level increases ($x > 0.1$), a slight growth of the diffraction intensity from the impurity phase can be observed, also indicating an increasing amount of impurity. However, an interesting question still exists: why an impurity phase would be commonly contained in electron-doped manganites but seldom reported in hole-doped manganites. The hole-doped manganites are usually doped with divalent elements such as Ca, Ba, and Sr, which are all rather reactive

metals under standard conditions. They have two electrons in their valence shell, so their energetically preferred state of achieving a filled electron shell is to lose two electrons to form doubly charged positive ions. Therefore, it is thought that these elements could react with MnO_2 or $MnCO_3$ compounds sufficiently during the solid state reaction, and little secondary phase can be found in hole-doped manganites. However, the tetravalent elements, which are used to form electron-doped manganites, have four electrons in the external shell and are relatively chemical stable. Doping tetravalent elements in the manganites seems harder than doing so with divalent elements. We think that might be the reason for the impurity phase contained in electron-doped manganites commonly. Further investigations of the mechanism of Hf doped manganites are under way. We are planning to do some other measurements to test whether any other impurity phases are mixed in LHMO.

In order to get further information on the low temperature magnetic properties of the LHMO system, the dynamic magnetic properties have been investigated via dc magnetization measurement, including relaxation and aging processes. The samples were first cooled down from a reference temperature in the PM state to the measuring temperature and kept for a waiting time t_w. Thereafter, a dc magnetic field was applied and the M(t) was recorded. Figure 6 displays the time dependence of M(t) measured in a field of 200 Oe at 10, 60, and 300 K after different waiting times t_w. After a magnetic field was applied, the increasing relaxation of the magnetization could be observed at 10 and 60 K, like in the FM phase. After the sample experiences a transition from FM to PM, the magnetization decreases with time due to the magnetic relaxation, as presented in Fig. 6(c). It is clearly found that the magnetization is strongly dependent on t_w, which demonstrates that the system possesses the aging process. Among the various physical models proposed to discuss the temperature dependence of magnetization, one of the most popular is a stretched exponential form as in[32]

$$M(t) = M_0 - M_r \exp\left[-\left(\frac{t}{t_w}\right)^{1-n}\right], \qquad (3)$$

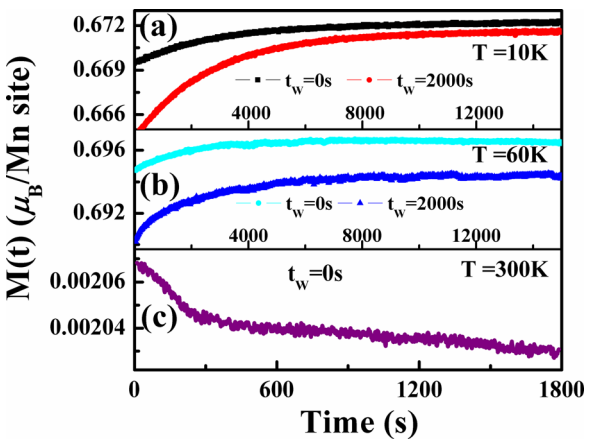

FIG. 6. (Color online) Time dependence of $M(t)/M_0$ (M_0 represents the maximum of the ZFC magnetization) of the LHMO(0.2) sample measured in 200 Oe at temperatures of 10, 60, and 300 K after different waiting times t_w.

TABLE I. The fitted parameters M_r/M_0, n, and τ_r of Eq. (3) for LHMO(0.2) fitted with the time dependence of the remanent magnetization data measured at 10 and 60 K.

T_m (K)	t_w (s)	M_r/M_0	n	τ_r (s)
10	0	0.0103	0.68	2847
10	2000	0.0039	0.63	3657
60	0	0.0052	0.47	1437
60	2000	0.0027	0.4	1803

where M_0 relates to the intrinsic FM component and M_r to the glassy component mainly contributing to the relaxation effects observed. We fitted $M(t)/M_0$ with Eq. (3). The fitting parameters are shown in Table I. M_r/M_0 depends on the temperature and decreases with increasing temperature. The waiting time t_w shows a significant effect on the magnetic relaxation, revealing an intrinsic aging process. This is a manifestation of the nonequilibrium nature of the spin-glass state. As we all know, to form the spin-glass state, two important factors must exist: disorder of sites or bonds, and completion between different magnetic phase interactions. Owing to the random substitution of La^{3+} with Hf^{4+}, there might exist disordered distributions of Mn^{2+} and Mn^{3+} ions in LHMO compounds. This could lead to a random distribution of the magnetic constants J_{FM} and J_{AFM}, as well as make magnetic frustration and FM clusters easy to form. Meanwhile, sthe ubstitution of different sizes of ions will result in lattice distortions, which might influence the FM DE and AFM SE interactions differently. As mentioned above, replacing La with Hf would lead to a decrease in Mn-O bond length and an increase of the Mn-O-Mn bond angle. Thus the enhanced lattice distortion would weaken the DE and favor SE interactions. This competition is sufficient to suppress long-range FM order and frustrated interaction among magnetic moments. DE and SE interactions would compete more strongly, with dependence on the structural distortion, giving rise to a magnetically disordered state. Therefore, we conclude that the coexistence and completion between the FM and AFM interactions, along with the randomness, would lead to the spin-glass state in LHMO compounds.

IV. CONCLUSION

The effects of tetravalent Hf doping in manganite oxides on the structural, magnetic, and transport properties are systematically studied in this paper. By measuring M-T and ρ-T curves of LHMO with different doping levels, we obtained the phase diagram of LHMO compounds ($0.05 \leq x \leq 0.3$) for the first time. It was found that the magnetic and electrical transport properties were strongly dependent on the Hf concentration. An abnormal enhancement of the magnetization in LHMO with $x \geq 0.1$ was observed at about 42 K and was attributed to the contribution of an unreacted MnO_2 impurity phase. There is coexistence of ferromagnetic and spin-glass states in the LHMO compounds at low temperature. Dynamic magnetic measurements in LHMO were carried out, including relaxation and aging studies, and further confirmed the nature of spin-glass behavior. Although it is fully

understood that the observed results call for more experiments and theoretical work, our results should be meaningful evidence of the electron-doped manganite family. Our study highlights the importance of double-exchange interactions and electronic correlation effects in understanding the occurrence of a ferromagnetic state accompanied with a spin-glass state in electron-doped manganites.

ACKNOWLEDGMENTS

This work has been supported by a grant from the Research Grant Council of Hong Kong (Project No. HKU702409P), the URC of the University of Hong Kong, the National Natural Science Foundation of China, and the National Basic Research Program of China.

[1]J. Fontcuberta, B. Martinez, A. Seffar, S. Pinol, J. L. GarciaMunoz, and X. Obradors, Phys. Rev. Lett. **76**, 1122 (1996).
[2]C. H. Booth, F. Bridges, G. H. Kwei, J. M. Lawrence, A. L. Cornelius, and J. J. Neumeier, Phys. Rev. Lett. **80**, 853 (1998).
[3]A. Urshibara, Y. Moritomo, T. Arima, A. Asamitsu, G. Kido, and Y. Tokura, Phys. Rev. B **51**, 14103 (1995).
[4]A. P. Ramirez, P. Schiffer, S.-W. Cheong, C. H. Chen, W. Bao, T. T. M. Palstra, P. L. Gammel, D. J. Bishop, and B. Zegarski, Phys. Rev. Lett. **76**, 3188 (1996).
[5]J. B. Philipp, L. Alff, A. Marx, and R. Gross, Phys. Rev. B **66**, 224417 (2002).
[6]E. Dagotto, New J. Phys. **7**, 67 (2005).
[7]H. Y. Hwang, S.-W. Cheong, N. P. Ong, and B. Batlogg, Phys. Rev. Lett. **77**, 2041 (1996).
[8]B. Dabrowski, X. Xiong, Z. Bukowski, R. Dybzinski, P. W. Klamut, J. E. Siewenie, O. Chmaissem, J. Shaffer, C. W. Kimball, J. D. Jorgensen, and S. Short, Phys. Rev. B **60**, 7006 (1999).
[9]J. Geck, P. Wochner, D. Bruns, B. Büchner, U. Gebhardt, S. Kiele, P. Reutler, and A. Revcolevschi, Phys. Rev. B **69**, 104413 (2004).
[10]A. J. Millis, B. I. Shraiman, and R. Mueller, Phys. Rev. Lett. **77**, 175 (1996).
[11]P. Schiffer, A. Ramirez, W. Bao, and S.-W. Cheong, Phys. Rev. Lett. **75**, 3336 (1995).
[12]E. J. Guo, J. Gao, and H. B. Lu, Appl. Phys. Lett. **98**, 081903 (2011).
[13]H. L. Ju, J. Gopalakrishnan, J. L. Peng, Q. Li, G. C. Xiong, T. Venkatesan, and R. L. Greene, Phys. Rev. B **51**, 6143 (1995).
[14]S. Das and P. Mandal, Indian J. Phys. **71**, 231 (1997); Z. Phys. B: Condens. Matter **7**, 104 (1997); P. Mandal and S. Das, Phys. Rev. B **56**, 15073 (1997).
[15]J. R. Gebhardt, S. Roy, and N. Ali, J. Appl. Phys. **85**, 5390 (1999).
[16]C. Mitra, P. Raychaudhuri, J. John, S. K. Dhar, A. K. Nigam, and R. Pinto, J. Appl. Phys. **89**, 524 (2001).
[17]H. Chou, C. B. Wu, S. G. Hsu, and C. Y. Wu, Phys. Rev. B **74**, 174405 (2006).
[18]P. Raychaudhuri, C. Mitra, P. D. A. Mann, and S. Wirth, J. Appl. Phys. **93**, 8328 (2003).
[19]G. T. Tan, S. Dai, P. Duan, Y. L. Zhou, H. B. Lu, and Z. H. Chen, Phys. Rev. B **68**, 014426 (2003).
[20]H. Z. Guo, Z. H. Chen, L. F. Liu, S. Ding, Y. L. Zhou, H. B. Lu, K. J. Jin, and B. L. Chen, Appl. Phys. Lett. **85**, 3172 (2004).
[21]J. Yang, Y. P. Lee, and Y. Li, Phys. Rev. B **76**, 054442 (2007).
[22]Z. W. Li, A. H. Morrish, and J. Z. Jiang, Phys. Rev. B **60**, 10284 (1999).
[23]J. Gao, S. Y. Dai, and T. K. Li, Phys, Rev. B **67**, 153403 (2003).
[24]P. Duan, S. Y. Dai, G. T. Tan, H. B. Lu, Y. L. Zhou, B. L. Cheng, and Z. H. Chen, J. Appl. Phys. **95**, 5666 (2004).
[25]J. Gao and L. Wang, Mater. Sci. Eng., B **144**, 97 (2004).
[26]L. Wang and J. Gao, J. Appl. Phys. **103**, 07F702 (2008).
[27]L. Wang and J. Gao, J. Appl. Phys. **105**, 07E514 (2009).
[28]L. Wang and J. Gao, J. Appl. Phys. **105**, 07C904 (2009).
[29]J. Yang, Y. P. Sun, W. H. Song, and Y. P. Lee, J. Appl. Phys. **100**, 123701 (2006).
[30]J. H. Kuo, H. U. Anderson, and D. M. Sparlin, J. Solid State Chem. **83**, 52 (1989).
[31]J. A. M. van Roosmalen and E. H. P. Cordfunke, J. Solid State Chem. **110**, 109 (1994).
[32]R. S. Freitas, L. Ghivelder, F. Damay, F. Dias, and L. F. Cohen, Phys. Rev. B **64**, 144404 (2001).